Performance Analysis of DWT-OFDM Diversity for Standard SV-Model Based UWB System

Article · December 2015

2 authors:

Chandrashekhar Deshmukh
Prof. Ram Meghe Institute of Technology & Research

V. T. Ingole
Dr.Rajendra Gode Institute of Tech. & Research, Amravti (MS) India

ISSN 2319 - 6629
Volume 4, No.1, December – January 2015
International Journal of Wireless Communications and Networking Technologies
Available Online at http://warse.org/pdfs/2014/ijwcnt02412015.pdf

Performance Analysis of DWT-OFDM Diversity for Standard SV-Model Based UWB System

C N Deshmukh[1], V T Ingole[2]
[1] Dept of Electronics & Telecommunication Engg., PRMIT&R, Badnera, Maharashtra-India,cndesh1968@gmail.com.
[2] Director, IBSS College of Engineering, Ghatkheda-Amravati, Maharashtra-India,vtingole@gmailcom

ABSTRACT

Recent generation communication system has a serious challenge of accommodating more users within limited allocated bandwidth without affecting the system performance. OFDM is used to cater for increased data rate of wireless medium with good performance. Diversity techniques play an important role in achieving higher performance level under imperfect channel condition. In this paper we propose a DWT-OFDM Diversity to achieve better performance in terms of SNR and bit error rate (BER) for SV model based standard UWB channel. The performance of different discrete wavelets are analyzed and compared with FFT based OFDM. The result indicates better BER performance in case of lower order wavelet.

Key words: BER, DWT, FFT, ISI, OFDM, SNR, SV Model, UWB

1. INTRODUCTION

Orthogonal Frequency Division Multiplexing (OFDM) constitute of combination of modulation and multiplexing wherein independent signal that are subset of main signal are multiplexed. The signal itself is first split into independent channel, modulated by data and further re-multiplexed to create OFDM carrier. As the subcarriers in OFDM are orthogonal, it allows simultaneous transmission of multiple sub carriers in a compact frequency space without interference. OFDM can provide large data rates even under channel impairment. Efficient compact spectral utilization can be achieved in OFDM scheme with help of minimally separated sub-carriers [3, 5]. Similarly OFDM scheme convert a broadband frequency selective channel into parallel flat fading narrow band sub channel.

In order to mitigate the problem of ISI (Inter symbol interference) caused by complex multipath wireless channel a cyclic prefix (CP) [4] is added to each symbol in OFDM system. The cyclic prefix causes ripples in the power spectral density of the UWB signal [2]. On the other hand wavelet based modulation satisfies orthogonality criterion.

We can derive benefits of OFDM even when traditional sinusoid carriers of FFT based OFDM are replaced with suitable wavelets. Wavelet based system have better to immunity to impulse and narrow band noises as compared to FFT OFDM [2, 4].

In addition to this wavelet based OFDM does not require any CP leading to increase in spectral efficiency, reduce complexity and better symbol rate. Discrete wavelet transform (DWT) are being considered as alternative platforms for replacing IFFT and FFT [6, 14-15]. It utilizes low pass filter and high pass filter, operating as Quadrature Mirror Filters (QMF) satisfying perfect reconstruction and ortho-normal properties. The purpose of this paper is to demonstrate the diversity advantage provided by use of DWT in lieu of FFT in OFDM system. DWT has been introduced as a highly efficient and flexible method for sub-band decomposition of signal.

Section 2 presents the traditional FFT OFDM and wavelet OFDM whereas **Section 3** describes the system and channel model. In **Section 4** simulation environment with result are discussed. **Section 5** concludes the paper

2. FFT OFDM AND WAVELET OFDM

2.1 FFT-OFDM

OFDM system is used as modulation method that divides a given bandwidth into multiple smaller sub-bands. In time domain, an N-point FFT OFDM system can be represented as:

$$s[n]=\frac{1}{\sqrt{N}}\sum_{k=0}^{N-1} S_k\, e^{j2\pi nk/N},\ n=0,1,2,\ldots\ldots N-1 \qquad (1)$$

Where s[n] is the discrete form of s(t), N is the number of sub-channels, $\frac{1}{\sqrt{N}}$ is a scaling factor with *n* as the index of the prevalent subcarrier. S_k is the BPSK mapped input symbol of k^{th} sub-channel. The number of FFT points used is same as the number of narrowband sub-channels over which the input symbols are multiplexed. Each of the resulting narrowband sub-channels is modulated by the mapped input bits. Cyclic prefix (CP) at least equal to the length of the channel response, *L* is pre-appended to each OFDM symbol to contest ISI. To account for the CP, Equation 1 can be expressed as [7]:

$$s[n]=\frac{1}{\sqrt{N}}\sum_{k=0}^{N-1} S_k\, e^{j2\pi nk/N},\ -N_g\leq n\leq N-1 \qquad (2)$$

In Equation 2, N_g denotes the length of CP pre-appended to every OFDM symbol.

2.2. Wavelet – OFDM

The discrete wavelet transform (DWT) can be used to study multicarrier systems as in [9]. It represents signals in time-frequency domain such that the signal exists neither purely in frequency domain nor purely in time domain. For a mapped input symbol S_k to be transformed by the DWT, the time domain output can be realized from [10];

$$s[n] = \sum_k \sum_{m=0}^{M-1} S_{k,n}\, \varphi_{m,n}(t) \tag{3}$$

where $S_{k,n}$ represents the n^{th} symbol which modulates the m^{th}-waveform of the k^{th}-constellation. $\varphi_{m,n}(t)$ represents the complex orthogonal DWT basis function similar to the traditional OFDM as:

$$\varphi_{m,n} = \begin{cases} 1 & n = m \\ 0 & elsewhere \end{cases} \tag{4}$$

where m and n are scales and shifts respectively. If n is the index of each discrete wavelet symbol s[n] of the continuous time symbol $s(t)$, then the wavelet transform is defined as [11]:

$$\Psi_{k,a}(t) = e^{j\pi t^2} \tag{5}$$

Now, let a continuous wavelet function is expressed as:

$$\Psi_{k,a}(t) = \frac{1}{\sqrt{k}}\Psi\left(\frac{t-a}{k}\right) \tag{6}$$

where k and a are the scaling and shifting parameters respectively and $\Psi(\cdot)$is called the mother wavelet. Then, from Equations 5 and 6 the resulting continuous transform can be represented as:

$$S_{CWT}(\tau, k) = \frac{1}{\sqrt{k}}\int_{-\infty}^{\infty} exp\left[i\pi\frac{(t-\tau)^2}{k^2}\right] s(t)dt \tag{7}$$

Equation 7 has the advantage of time and frequency diversities unlike the FFT transform that has only frequency diversity advantage. In fact, it has been explored that orthogonal wavelet-based OFDM is more robust to ICI and ISI problems than the FFT-based OFDM [1, 12-13]. Absence of CP in wavelet OFDM unlike that in FFT OFDM, provides for additional 25% spectral efficiency.

3. SYSTEM AND CHANNEL MODEL

3.1 FFT OFDM model

The OFDM system model described below is utilized for both FFT-OFDM and DWT-OFDM. The input binary data is generated randomly as bit stream b. It is processed using BPSK modulator to map the input data into symbols X_m. These symbols are now passed through IFFT block to perform IFFT operation to generate N parallel data streams. Its output in discrete time domain is given by [5],

$$X_{k(n)} = \frac{1}{\sqrt{N}}\sum_{i=0}^{N-1} X_m(i)e^{\left(\frac{j2\pi ni}{N}\right)} \tag{8}$$

The cyclic prefix is now appended to transformed output (X_k). The cyclic prefix (CP) is added before transmission, to moderate ISI effect. This OFDM symbol is passed through standard UWB channel. At the receiver, the reverse operation is carried out to obtain the original data back. The CP is removed and processed in the FFT block and finally passed through demodulator for data recovery. The output of the FFT in frequency domain is given by,

$$Y_{m(i)} = \sum_{n=0}^{N-1} Y_{k(n)}e^{\left(\frac{-j2\pi ni}{N}\right)} \tag{9}$$

3.2 DWT OFDM Model

In DWT OFDM, at the transmitter the input data b maps on to BPSK modulator, thereby converting data b_k into symbols $X_{m(i)}$. Each $X_{m(i)}$ is first converted to serial representation having a vector XX which will next be transposed into CA. Then, the signal is up-sampled (zero padding) and filtered by the LPF coefficients or approximated coefficients. Since our aim is to have low frequency signals, the modulated signals XX perform circular convolution with LPF filter whereas the HPF filter also perform the convolution with zeroes padding signals CD respectively. Note that the HPF filter contains detailed coefficients or wavelet coefficients. This data is given as an input to IDWT block wherein a particular wavelet is chosen for simulation. At the receiver, DWT and PSK demodulator (BPSK) are used to recover back the data [5].

3.3 Channel Model

The SV model distinguishes between "cluster arrival rates" and "ray arrival rates". The first cluster starts by definition at time t=0, and the following rays are arriving with a rate given by a Poisson process with rate λ. The power of those rays decays exponentially with increasing delay from the first ray. The "cluster arrival rate", which is smaller than the ray arrival rate, in turn determines when the next cluster has its origin. The rays within that cluster are again a Poisson process with rate λ[16].
Mathematically, the impulse response is described as

$$h_i(t) = X_i \sum_{l=0}^{L}\sum_{k=0}^{K} \propto_{k,l}^{i}\ \delta(t - T_l^i - \tau_{k,l}^i)$$

where

- $\{\propto_{k,l}^{i}\}$ are the multipath gain coefficients,
- $\{T_l^i\}$ is the delay of the l^{th} cluster,
- $\{\tau_{k,l}^i\}$ is the delay of the k^{th} multipath component relative to the l^{th} cluster arrival time (T_l^i),
- $\{X_i\}$ represents the log-normal shadowing, and i refers to the i^{th} realization.

Defining

- T_l = the arrival time of the first path of the l-th cluster;
- $\tau_{k,l}$ = the delay of the k-the path within the l-th cluster relative to the first path arrival time, T_l;
- Λ= cluster arrival rate;
- λ=ray arrival rate, i.e., the arrival rate of path within each cluster.

By definition, $\tau_{0,l} = 0$. The distribution of cluster arrival time and the ray arrival time are given by

$$p\,(T_l|T_{l-1}) = \Lambda \exp[-\Lambda\,(T_l - T_{l-1})], \qquad l > 0$$

$$p\,(\tau_{k,l}|\tau_{(k-l),l}) = \lambda \exp[-\lambda\,(\tau_{k,l} - \tau_{(k-l),l})], \qquad k > 0$$

The channel coefficients are defined as a product of small-scale and large-scale fading coefficients,

$$\text{i.e.,}\quad \alpha_{k,l} = p_{k,l}\,\xi_l\,\beta_{k,l},$$

The behavior of the (averaged) power delay profile is

$$E[|\xi_l\,\beta_{k,l}|^2] = \Omega_0\, e^{-T_l/\Gamma}\, e^{-\tau_{k,l}/\gamma}$$

which reflects the exponential decay of each cluster, as well as the decay of the total cluster power with delay.

In the above equations, ξ_l reflects the fading associated with the l^{th} cluster, and $\beta_{k,l}$ corresponds to the fading associated with the k^{th} ray of the l^{th} cluster.

Finally, since the log-normal shadowing of the total multipath energy is captured by the term, X_i, the total energy contained in the terms $\{\propto^i_{k,l}\}$ is normalized to unity for each realization. This shadowing term is characterized by the following:

$$20\log10(X_i) \propto \text{Normal}(0, \sigma_x^2).$$

4. SIMULATION ENVIRONMENT, RESULT AND DISCUSSION

Following UWB channels parameters were consider for performance analysis.

Channel Type	Cluster arrival rate	Ray arrival rate	Cluster decay factor	Ray decay factor
CM1 (LOS)	0.0233	2.5	7.1	4.3
CM2 (NLOS)	0.4	0.5	5.5	6.7
CM3 (NLOS)	0.0667	2.1	14.0	7.9
CM4 (25 ns RMS delay spread bad multipath)	0.0667	2.1	24.0	12.0

OFDM with 128 subcarriers and 256 subcarriers are being considered in simulation [8]. Simulation has been carried out for 54 wavelet namely Haar, db1 to db 10, sym 1 to sym 8, coif 1 to coif 5, bio-orthogonal family and reverse bio-orthogonal family.

Channel Type	SD of impulse response	SD for cluster fading	SD for Ray fading
CM1 (LOS)	3.0	1.414	1.414
CM2 (NLOS)	3.0	1.414	1.414
CM3 (NLOS)	3.0	1.414	1.414
CM4 (25 ns RMS delay spread bad multipath)	3.0	1.414	1.414

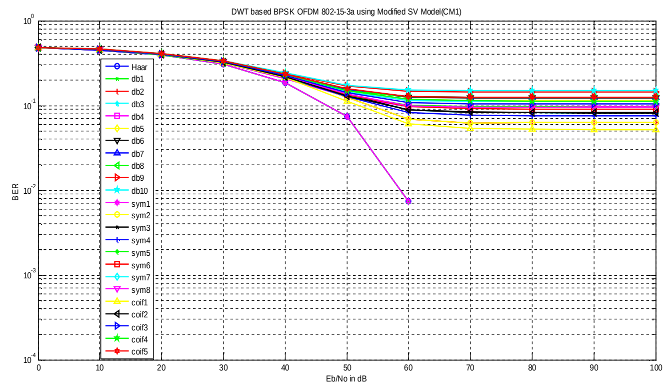

Figure(a.1):DWT-OFDM(128) for SV Model std. UWB Chaanel CM1

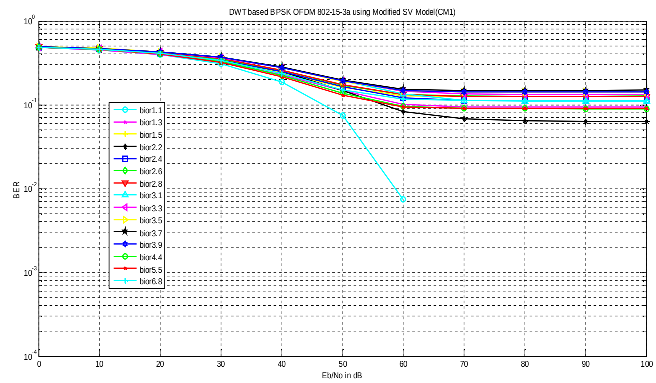

Figure(a.2):DWT-OFDM(128) for SV Model std. UWB Chaanel CM1

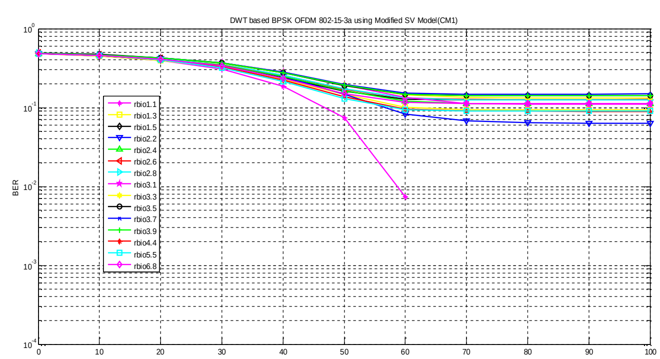

Figure(a.3):DWT-OFDM(128) for SV Model std. UWB Chaanel CM1

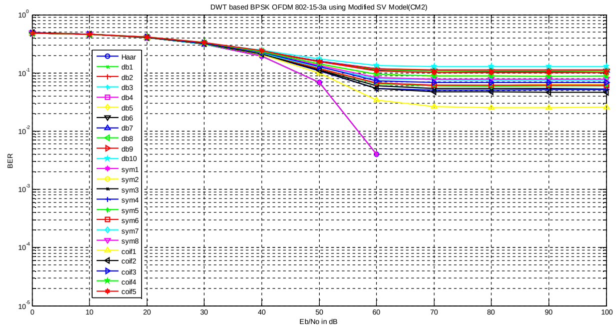

Figure(b.1):DWT-OFDM(128) for SV Model std. UWB Chaanel CM2

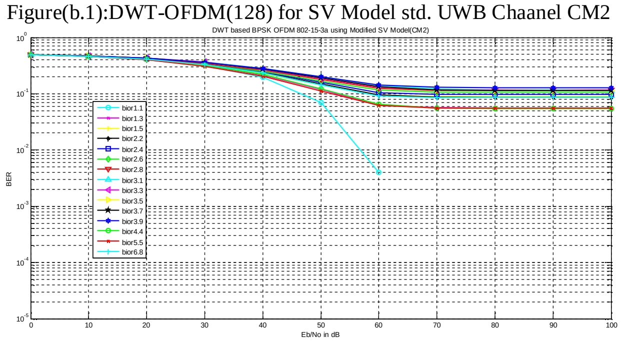

Figure(b.2):DWT-OFDM(128) for SV Model std. UWB Chaanel CM2

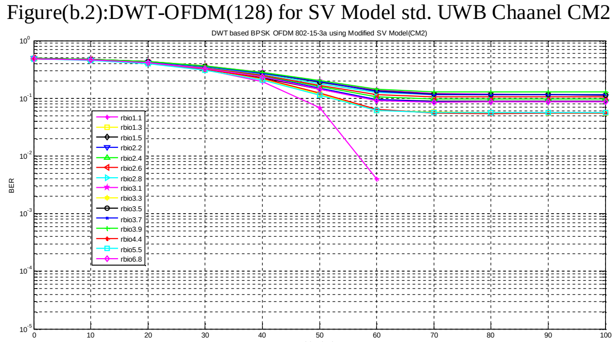

Figure(b.3):DWT-OFDM(128) for SV Model std. UWB Chaanel CM2

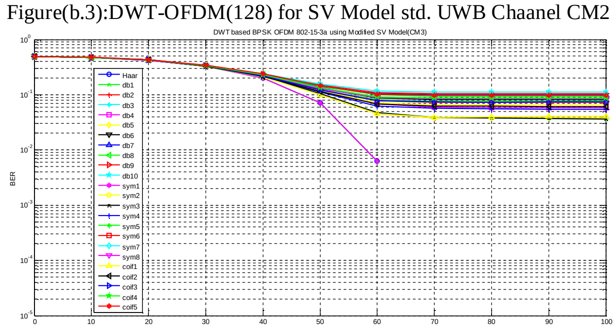

Figure(c.1):DWT-OFDM(128) for SV Model std. UWB Chaanel CM3

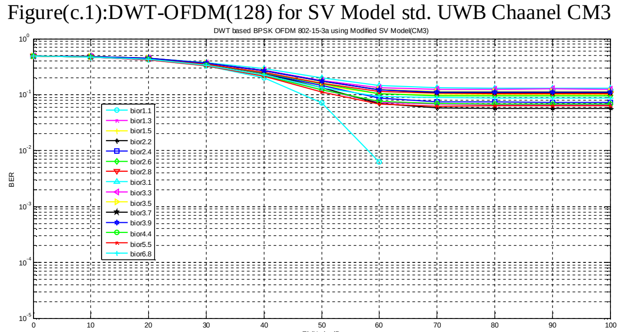

Figure(c.2):DWT-OFDM(128) for SV Model std. UWB Chaanel CM3

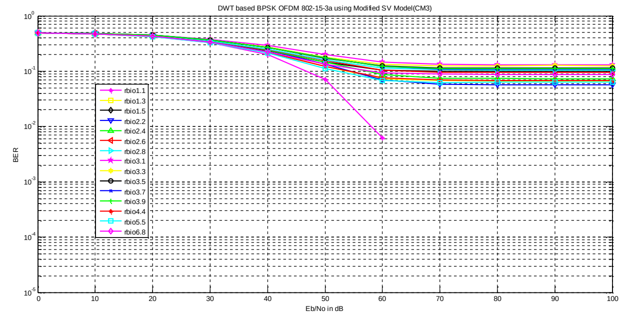

Figure(c.3):DWT-OFDM(128) for SV Model std. UWB Chaanel CM3

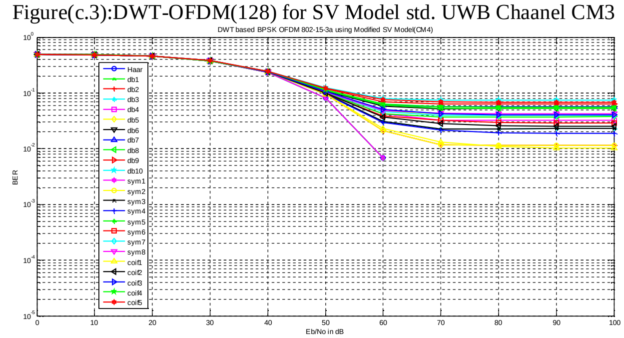

Figure(d.1):DWT-OFDM(128) for SV Model std. UWB Chaanel CM4

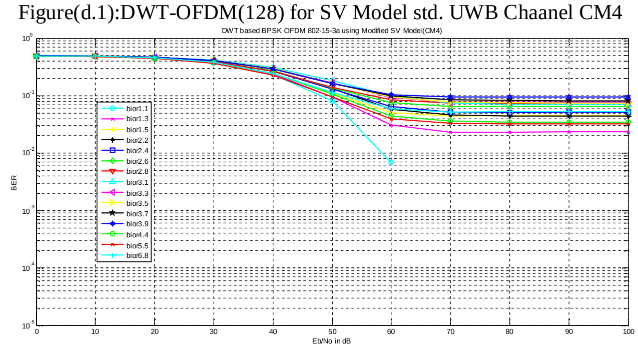

Figure(d.2):DWT-OFDM(128) for SV Model std. UWB Chaanel CM4

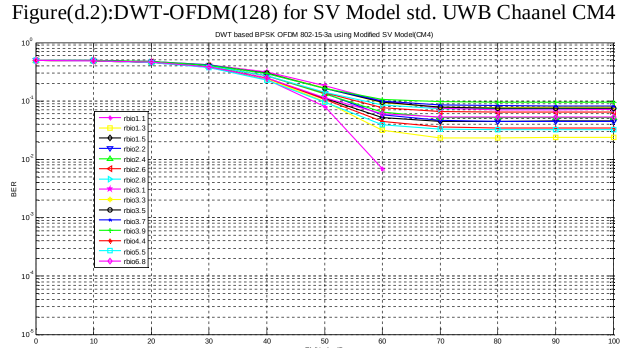

Figure(d.3):DWT-OFDM(128) for SV Model std. UWB Chaanel CM4

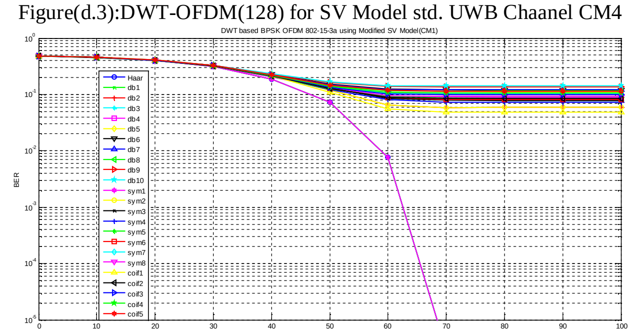

Figure(e.1):DWT-OFDM(256) for SV Model std. UWB Chaanel CM1

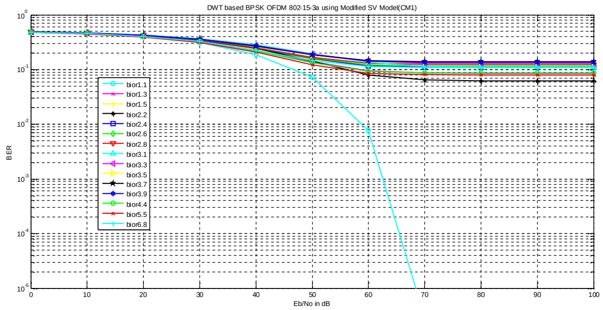

Figure(e.2):DWT-OFDM(256) for SV Model std. UWB Chaanel CM1

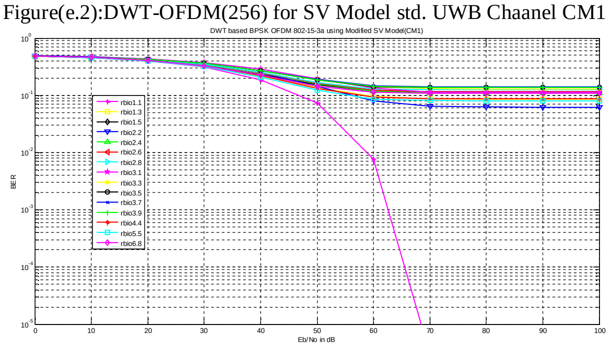

Figure(e.3):DWT-OFDM(256) for SV Model std. UWB Chaanel CM1

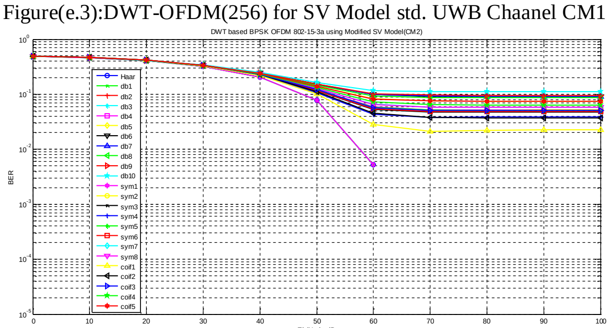

Figure(f.1):DWT-OFDM(256) for SV Model std. UWB Chaanel CM2

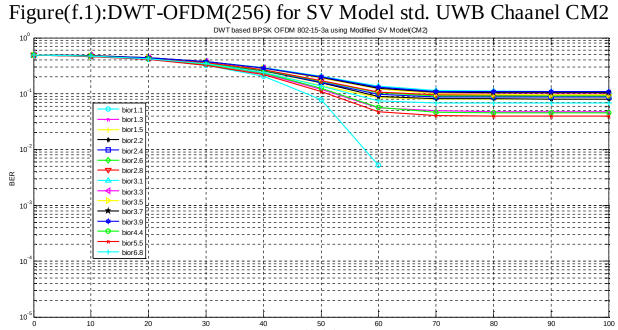

Figure(f.2):DWT-OFDM(256) for SV Model std. UWB Chaanel CM2

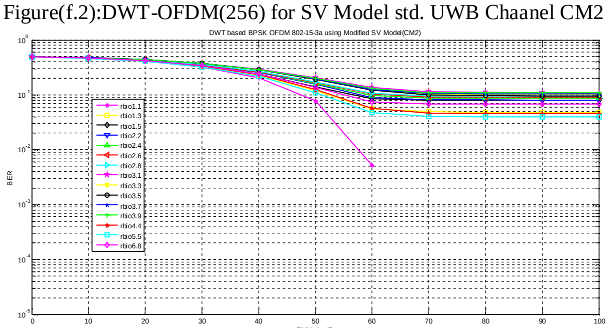

Figure(f.3):DWT-OFDM(256) for SV Model std. UWB Chaanel CM2

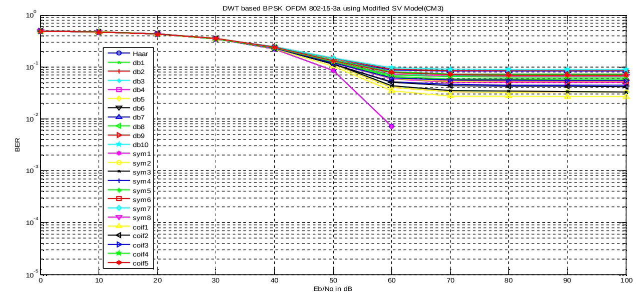

Figure(g.1):DWT-OFDM(256) for SV Model std. UWB Chaanel CM3

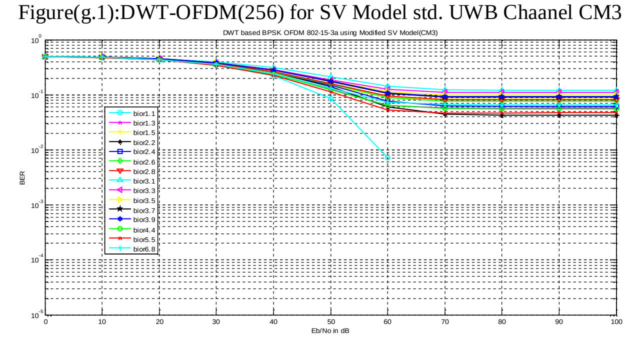

Figure(g.2):DWT-OFDM(256) for SV Model std. UWB Chaanel CM3

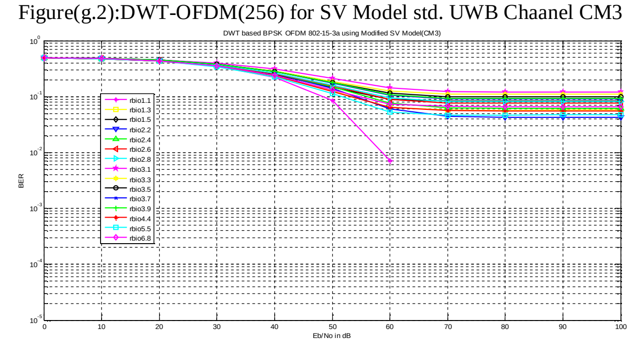

Figure(g.3):DWT-OFDM(256) for SV Model std. UWB Chaanel CM3

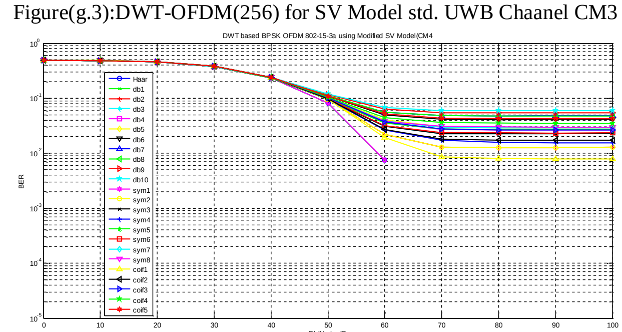

Figure(h.1):DWT-OFDM(256) for SV Model std. UWB Chaanel CM4

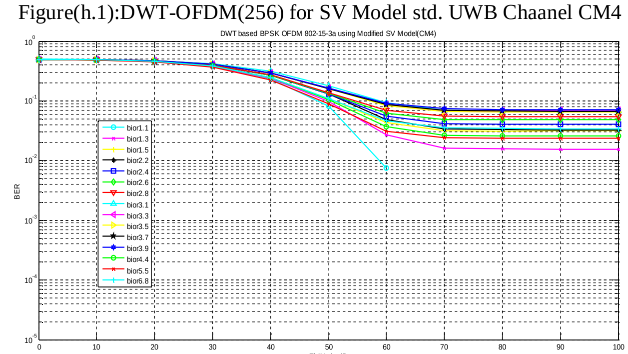

Figure(h.2):DWT-OFDM(256) for SV Model std. UWB Chaanel CM4

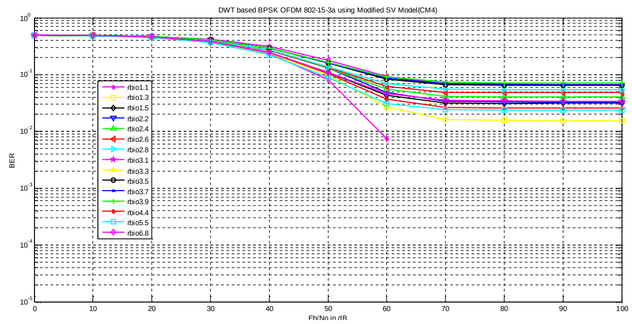

Figure(h.3):DWT-OFDM(256) for SV Model std. UWB Chaanel CM4

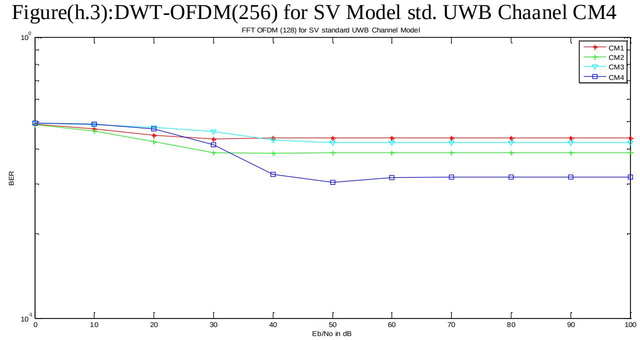

Figure (i.1): FFT-OFDM(128) for SV Model std UWB Channel

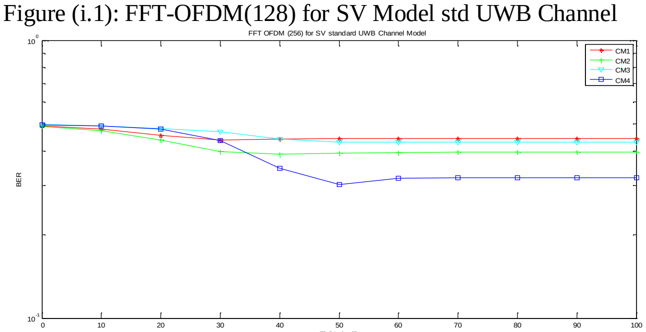

Figure (i.2): FFT-OFDM (256) for SV Model std UWB Channel

Figure a.1 to figure d.3 show the BER performance for different wavelets over different channels for DWT-OFDM with 128 sub-carriers. Figure e.1 to figure h.3 show the BER performance for different wavelets over different channels for DWT-OFDM with 256 sub-carriers. Figure i.1 and figure i.2 show the BER performance for FFT-OFDM. Simulation results indicate that lower order wavelets like Haar, db1, sym1, bior1.1 and rbior1.1 show good performances for all channel models. The results for other wavelet types do not indicate appreciable improved performance but exhibit much better performance as compared to FFT OFDM. Similarly the performance for OFDM with 128 subcarriers and 256 subcarriers is more or less similar. The results indicate good BER performance for Eb/No (SNR) above 60 dB.

5. CONCLUSION

This paper, presents an effective implementation of DWT OFDM diversity and its comparison with FFT OFDM. Wavelet based analysis is more immune to impulse and narrow band noise as compared to Fourier based OFDM resulting in improved spectral efficiency. Results reveal that DWT OFDM has robust ability to repel inter carrier interference and noise. Wavelet provides advantage of time and frequency diversities unlike FFT and hence suitable for fast fading UWB channels.

REFERENCES

1. B. G. Negash and H. Nikookar. **Wavelet-Based Multicarrier Transmission Over Multipath Wireless Channels**, IEE Electronics Letters, vol. 36, **(2000)** October, pp. 1787-1788.
2. A. R. Lindsey. **Generalized Orthogonally Multiplexed Communication via Wavelet Packet Bases**, Ph.D. Thesis, Ohio University, **(1995)**.
3. A. Batra, J. Balakrishnan, G. R. Aiello, J. R. Foerster and A. Dabak. **Design of a multiband OFDM system for realistic UWB channel environments**, IEEE Transactions on Microwave Theory and Techniques, vol. 52, no. 9, **(2004)** September, pp. 2123–2139.
4. Md. Mahmudul Hasan. **Performance Comparison of Wavelet and FFT Based Multiuser MIMO OFDM over Wireless Rayleigh Fading Channel**, International Journal of Energy, Information and Communications Vol. 3, Issue 4, November, 2012.
5. Mrs. Veena M.B & Dr. M.N.Shanmukha Swamy. **Performance analysis of DWT based OFDM over FFT based OFDM and implementing on FPGA**, International Journal of VLSI design & Communication Systems (VLSICS) Vol.2, No.3, September 2011.
6. B. Negash and H. Nikookar. **Wavelet based OFDM for wireless channels**, in IEEE VTS 53rd Vehicular Technology Conference, 2001. VTC 2001 Spring. 2001, pp. 688-691.
7. Kelvin O. O. Anoh, Raed A. A. Abd-Alhameed, Michael Chukwu, Mohammed Buhari and Steve M. R. Jones. **Towards a Seamless Future Generation Network for High Speed Wireless Communications**, (IJACSA) International Journal of Advanced Computer Science and Applications, Vol. 4, No. 9, 2013.
8. Yong Soo Cho, Jaekwon Kim, Won Young Yang and Chung G. Kang. **MIMO – OFDM wireless communication with MATLAB**, John Wiley and Sons (Asia) Pvt. Ltd.,2010.
9. O. O. Anoh, N. T. Ali, R. Abd-Alhameed, S. M. Jones, and Y. A. Dama. **On the performance of DWT and WPT modulation for multicarrier systems**, in 2012 IEEE 17th International Workshop on Computer Aided Modeling and Design of Communication Links and Networks (CAMAD), 2012, pp. 348-352.
10. A. Jamin and P. Mahonen. **Wavelet packet modulation for wireless communications**, Wireless Communications and Mobile Computing, vol. 5, pp. 123-137, 2005.
11. H. M. Ozaktas, B. Barshan, D. Mendlovic, and L. Onural. **Convolution, filtering, and multiplexing in fractional Fourier domains and their relation to chirp and wavelet transforms**, JOSA A, vol. 11, 1994, pp. 547-559.
12. B. Negash and H. Nikookar. **Wavelet based OFDM for wireless channels**, in IEEE VTS 53rd Vehicular Technology Conference, 2001. VTC 2001 Spring. 2001, pp. 688-691.
13. Y. Zhang and S. Cheng. **A novel multicarrier signal transmission system over multipath channel of**

low-voltage power line, IEEE Transactions on Power Delivery, vol. 19, pp. 1668-1672, 2004.

14. K. Abdullah and Z. M. Hussain. **Studies on DWT-OFDM and FFT-OFDM Systems**, IEEE International Conference on Communication, Computer and Power, February 15-18, 2009.
15. W. Saad, N. El-Fishawy, S. EL-Rabaie, and M. Shokair. **An Efficient Technique for OFDM System Using Discrete Wavelet Transform**, Springer-Verlag Berlin Heidelberg, pp. 533–541, 2010.
16. Jeffrey R. Foerster, Marcus Pendergrass and Andreas F. Molisch. **A Channel Model for Ultra wideband Indoor Communication**, Mitsubishi Electric Research Laboratories, TR2004-074 October 2003.